

Optimized Training Design for Multi-Antenna Wireless Energy Transfer in Frequency-Selective Channel

Yong Zeng and Rui Zhang

Department of Electrical and Computer Engineering, National University of Singapore

Email: {elezeng, elezhang}@nus.edu.sg

Abstract

This paper studies the optimal training design for a multiple-input single-output (MISO) wireless energy transfer (WET) system in frequency-selective channels, where the frequency-diversity and energy-beamforming gains can be both achieved by properly learning the channel state information (CSI) at the energy transmitter (ET). By exploiting channel reciprocity, a two-phase channel training scheme is proposed to achieve the diversity and beamforming gains, respectively. In the first phase, pilot signals are sent from the energy receiver (ER) over a selected subset of the available frequency sub-bands, through which the sub-band that exhibits the largest sum-power over all the antennas at the ET is determined and its index is sent back to the ER. In the second phase, the selected sub-band is further trained for the ET to estimate the multi-antenna channel and implement energy beamforming. We propose to maximize the *net* energy harvested at the ER, which is the total harvested energy offset by that used for the two-phase channel training. The optimal training design, including the number of sub-bands trained and the energy allocated for each of the two phases, is derived.

I. INTRODUCTION

Wireless energy transfer (WET) has drawn significant interests recently due to its great potential to provide cost-effective and reliable power supplies for energy-constrained wireless networks [1]. One enabling technique of WET for long-range applications (say up to tens of meters) is via radio-frequency (RF) or microwave propagation, where dedicated energy-bearing signals are transmitted from the energy transmitter (ET) for the energy receiver (ER) to harvest the RF energy (see e.g. [2] and references therein). To overcome the significant power attenuation over distance, employing multiple antennas at the ET and advanced beamforming techniques to efficiently direct wireless energy to the destined ER, termed *energy beamforming*, is an essential technique for WET [3]. Similar to the emerging massive multiple-input multiple-output (MIMO) enabled wireless communications (see e.g. [4] and references therein), by equipping a very large number of antennas at the ET, enormous energy beamforming gain can be achieved; hence, the end-to-end energy transfer efficiency can be greatly enhanced.

On the other hand, for MIMO WET in a wide-band regime over frequency-selective channels, the frequency-diversity gain can also be exploited to further enhance the energy transfer efficiency, by transmitting more power over the sub-band with higher channel gain. WET in single-antenna or single-input single-output (SISO) frequency-selective channels has been studied in [5]–[7] under the more general setup of simultaneous wireless information and power transfer (SWIPT), where perfect channel state information (CSI) is assumed at the transmitter.

In practice, both the energy-beamforming and frequency-diversity gains in MIMO WET over frequency-selective channels can be achieved, but crucially depend on the available CSI at the ET, which needs to be practically obtained at the cost of additional time and energy consumed. Similar to wireless communication, a direct approach to obtain CSI is by sending pilot signals from the ET to the ERs, each of which estimates the corresponding channel and then sends the estimated channel back to the ET via a feedback channel [8], [9]. However, since the training overhead increases with the number of antennas M at the ET, this method is not suitable when M is large. In [10], a new channel-learning design to cater for the practical RF energy harvesting circuitry at the ER has been proposed. However, the training overhead still increases quickly with M , and can be prohibitive for large M . In [11], by exploiting channel reciprocity between the forward (from the ET to the ER) and reverse (from the ER to the ET) links, we have proposed an alternative channel-learning scheme for WET based on the reverse-link training, which is more efficient since the training overhead becomes independent of M . However, the proposed design in [11] applies only for narrowband flat-fading channels instead of the more complex broadband frequency-selective fading channels, which motivates this work.

In this paper, we consider a MISO point-to-point WET system over frequency-selective fading channels. To exploit both the frequency-diversity and energy-beamforming gains, we propose a two-phase channel training scheme by exploiting the channel reciprocity. In the first phase, pilot signals are sent from the ER over a selected subset of the available frequency sub-bands, each over an independent flat-fading channel. Based on the received total energy over all the antennas at the ET over each of the trained sub-bands, the ET determines the sub-band that has the largest energy and sends its index to the ER. In the second phase, the selected sub-band is further trained by the ER, so that the ET obtains an estimate of the exact MISO channel over this sub-band to implement energy beamforming. Due to the limited energy harvested at the ER, the training design needs to achieve a good balance between exploiting the diversity versus beamforming gains, yet without consuming excessive energy at the ER. Therefore, we propose to maximize the *net* energy harvested at the ER, which is the total harvested energy offset by that used for both phases of channel training. The optimal training design, including the number of sub-bands trained and the energy allocated for each of the two training phases, is derived. Simulation results are provided to validate our analysis.

II. SYSTEM MODEL

We consider the MISO point-to-point WET system in frequency-selective channel, where an ET with $M \geq 1$ antennas is employed to deliver wireless energy to a single-antenna ER. We assume that the total bandwidth is B

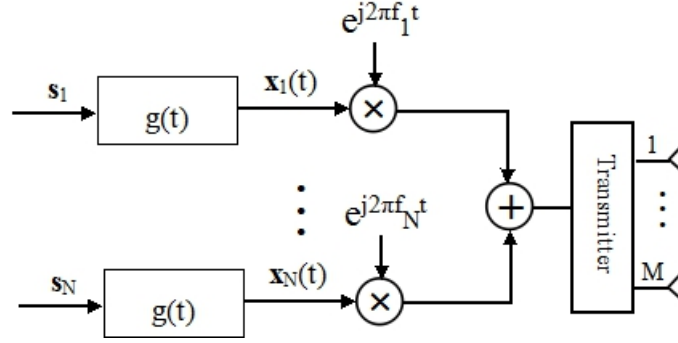


Fig. 1. Schematics of a multi-antenna multi-band wireless energy transmitter.

Hz, which is equally divided into N orthogonal sub-bands with the n th sub-band centered at frequency f_n and of bandwidth $B_s = B/N$. We assume that $B_s \ll B_c$, where B_c denotes the channel coherence bandwidth, so that the channel between the ET and ER experiences frequency flat-fading within each sub-band. Denote $\mathbf{h}_n \in \mathbb{C}^{M \times 1}$, $n = 1, \dots, N$, as the baseband equivalent MISO channel from the ET to the ER in the n th sub-band. We assume a quasi-static Rayleigh fading model, where \mathbf{h}_n remains constant within each block of $T \ll T_c$ seconds, with T_c denoting the channel coherence time, but can vary from one block to another. Furthermore, the elements in \mathbf{h}_n are modeled as independent and identically distributed (i.i.d.) zero-mean circularly symmetric complex Gaussian (CSCG) random variables with variance β , i.e.,

$$\mathbf{h}_n \sim \mathcal{CN}(\mathbf{0}, \beta \mathbf{I}_M), \quad n = 1, \dots, N, \quad (1)$$

where β models the large-scale fading due to shadowing as well as the distance-dependent path loss.

Within each block of T seconds, i.e., $0 \leq t \leq T$, the input-output relation for the forward link energy transmission can be expressed as

$$y_n(t) = \mathbf{h}_n^H \mathbf{x}_n(t) + z_n(t), \quad n = 1, \dots, N, \quad (2)$$

where $y_n(t)$ denotes the received signal at the ER; $\mathbf{x}_n(t) \in \mathbb{C}^{M \times 1}$ denotes the baseband energy-bearing signals transmitted by the ET in the n th sub-band; and $z_n(t)$ denotes the additive noise at the ER. Different from wireless communication where random signals need to be transmitted to convey information, $\mathbf{x}_n(t)$ in (2) is designated only for energy transmission and thus can be chosen to be deterministic. Denote by P_f the total transmit power constraint at the ET over the N sub-bands. We thus have

$$\frac{1}{T} \sum_{n=1}^N \int_0^T \|\mathbf{x}_n(t)\|^2 dt \leq P_f. \quad (3)$$

At the ER, the incident RF power captured by the antenna is converted to usable direct current (DC) power by a device called rectifier [12]. By ignoring the energy harvested from the background noise which is practically small, the total harvested energy over all N sub-bands during one block can be expressed as [3]

$$Q = \eta \sum_{n=1}^N \int_0^T |\mathbf{h}_n^H \mathbf{x}_n(t)|^2 dt, \quad (4)$$

where $0 < \eta \leq 1$ denotes the energy harvesting efficiency at the ER. Without loss of generality, $\mathbf{x}_n(t)$ can be expressed as (see Fig. 1 for the transmitter schematics)

$$\mathbf{x}_n(t) = \mathbf{s}_n g(t), \quad 0 \leq t \leq T, \quad n = 1, \dots, N, \quad (5)$$

where $\mathbf{s}_n \in \mathbb{C}^{M \times 1}$, and $g(t)$ represents the pulse-shaping waveform (e.g., raised cosine pulse) with normalized power, i.e., $\frac{1}{T} \int_0^T |g(t)|^2 dt = 1$. Note that the bandwidth of $g(t)$, which is approximately equal to $1/T$, needs to be no larger than B_s . We thus have

$$\frac{1}{T_c} \ll \frac{1}{T} < B_s \ll B_c, \quad (6)$$

or $T_c B_c \gg 1$, i.e., a so-called ‘‘under-spread’’ wide-band fading channel is assumed.

From (5), the power constraint in (3) can be rewritten as $\sum_{n=1}^N \|\mathbf{s}_n\|^2 \leq P_f$, and the harvested energy Q in (4) can be expressed as $Q = \eta T \sum_{n=1}^N |\mathbf{h}_n^H \mathbf{s}_n|^2$. In the ideal case with perfect CSI, $\{\mathbf{h}_n\}_{n=1}^N$, at the ET, the optimal design of $\{\mathbf{s}_n\}_{n=1}^N$ that maximizes Q can be obtained by solving the following problem

$$\begin{aligned} & \max \eta T \sum_{n=1}^N |\mathbf{h}_n^H \mathbf{s}_n|^2 \\ & \text{subject to } \sum_{n=1}^N \|\mathbf{s}_n\|^2 \leq P_f. \end{aligned} \quad (7)$$

It can be easily shown that the optimal solution to problem (7) is

$$\mathbf{s}_n = \begin{cases} \sqrt{P_f} \frac{\mathbf{h}_n}{\|\mathbf{h}_n\|}, & \text{if } n = \arg \max_{n'=1, \dots, N} \|\mathbf{h}_{n'}\|^2, \\ \mathbf{0}, & \text{otherwise.} \end{cases} \quad (8)$$

The resulting harvested energy can be expressed as

$$Q_{\max} = \eta T P_f \max_{n=1, \dots, N} \|\mathbf{h}_n\|^2. \quad (9)$$

It is observed from (8) that for a MISO multi-band WET system with the sum-power constraint, the optimal energy transmission scheme allocates all the available power to the sub-band with the largest MISO channel power. As a result, all the other sub-bands can be used for other applications such as communication. The solution given in (8) also indicates that for the selected sub-band, maximum ratio transmission (MRT) should be performed across different transmit antennas at the ET to achieve the maximum energy beamforming gain.

In practice, the CSI $\{\mathbf{h}_n\}_{n=1}^N$ needs to be estimated at the ET. By exploiting channel reciprocity, we propose a two-phase channel training scheme, as illustrated in Fig. 2. The first phase corresponds to the first $\tau_1 < T$ seconds of each block, where pilot signals are sent by the ER to the ET over N_1 out of the N available sub-bands, each with energy E_1 . By estimating the received energy over all M antennas at the ET over each of the N_1 trained sub-bands (whose indices are assumed to be known at the ET), the ET determines the sub-band with the largest power gain $\|\mathbf{h}_{n^*}\|^2$, and sends the index n^* to the ER. In the second phase of $\tau_2 < T - \tau_1$ seconds, additional training signal is sent by the ER in sub-band n^* with energy E_2 . The ET then obtains an estimate of the exact

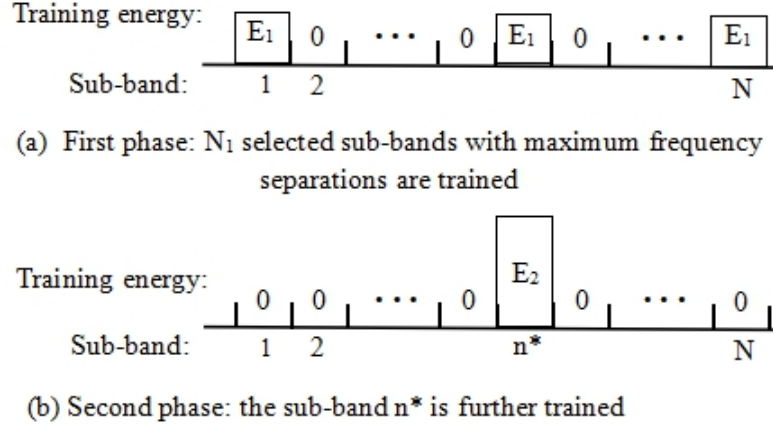


Fig. 2. Two-phase channel training for multi-antenna multi-band wireless energy transfer.

MISO channel \mathbf{h}_{n^*} , based on which MRT-based energy beamforming is applied during the remaining $T - \tau_1 - \tau_2$ seconds of each block. The proposed two-phase training scheme is elaborated in more details in the next section.

III. PROBLEM FORMULATION

A. Two-Phase Training

1) *Training Phase I*: Denote by $\mathcal{N}_1 \subset \{1, \dots, N\}$ with $|\mathcal{N}_1| = N_1$ the N_1 selected sub-bands trained in phase I. To maximize the frequency-diversity gain, the sub-bands with the maximum frequency separations are selected in \mathcal{N}_1 so that their channels are most likely to be independent (see Fig. 2(a)), e.g., if $N_1 = 2$, we have $\mathcal{N}_1 = \{1, N\}$. The received training signals at the ET can be written as

$$\mathbf{r}_n^I(t) = \sqrt{E_1} \mathbf{h}_n \phi_n(t) + \mathbf{w}_n^I(t), \quad 0 \leq t \leq \tau_1, \quad n \in \mathcal{N}_1, \quad (10)$$

where E_1 denotes the training energy used by the ER for each trained sub-band; $\phi_n(t)$ represents the training waveform for sub-band n with normalized energy, i.e., $\int_0^{\tau_1} |\phi_n(t)|^2 dt = 1, \forall n$; and $\mathbf{w}_n^I(t) \in \mathbb{C}^{M \times 1}$ represents the additive white Gaussian noise received at the ET with power spectrum density N_0 . The total energy consumed at the ER for channel training in this phase is

$$E_{\text{tr}}^I = \sum_{n \in \mathcal{N}_1} \int_0^{\tau_1} |\sqrt{E_1} \phi_n(t)|^2 dt = E_1 N_1. \quad (11)$$

At the ET, the received training signal is first separated over different selected sub-bands; then each $\mathbf{r}_n^I(t)$ passes through a matched filter to get

$$\mathbf{y}_n^I = \int_0^{\tau_1} \mathbf{r}_n^I(t) \phi_n^*(t) dt = \sqrt{E_1} \mathbf{h}_n + \mathbf{z}_n^I, \quad n \in \mathcal{N}_1, \quad (12)$$

where $\mathbf{z}_n^I \sim \mathcal{CN}(\mathbf{0}, N_0 \mathbf{I}_M)$ denotes the i.i.d. additive Gaussian noise vector. Based on (12), the ET determines the sub-band n^* that has the largest received energy as

$$n^* = \arg \max_{n \in \mathcal{N}_1} \|\mathbf{y}_n^I\|^2. \quad (13)$$

The ET then sends the index n^* to the ER.

2) *Training Phase II*: In the second phase of τ_2 seconds, additional pilot signal $u(t)$ is transmitted by the ER over sub-band n^* with energy E_2 . With similar processing as that in phase I, the received signal at the ET over sub-band n^* is

$$\mathbf{y}_{n^*}^{\text{II}} = \sqrt{E_2} \mathbf{h}_{n^*} + \mathbf{z}_{n^*}^{\text{II}}, \quad (14)$$

where $\mathbf{z}_{n^*}^{\text{II}} \sim \mathcal{CN}(\mathbf{0}, N_0 \mathbf{I}_M)$. The ET then performs the linear minimum mean-square error (LMMSE) based estimation for \mathbf{h}_{n^*} based on $\mathbf{y}_{n^*}^{\text{II}}$.¹ To obtain the optimal LMMSE estimator, we first provide the following lemma.

Lemma 1: Given that \mathbf{h}_n and \mathbf{h}_m are independent $\forall n, m \in \mathcal{N}_1$ and $n \neq m$, the average power of the MISO channel \mathbf{h}_{n^*} over the selected sub-band n^* can be expressed as

$$R_h(N_1, E_1) \triangleq \mathbb{E} \left[\|\mathbf{h}_{n^*}\|^2 \right] = \frac{\beta^2 E_1 G(N_1, M) + \beta N_0 M}{\beta E_1 + N_0}, \quad (15)$$

where $G(N_1, M) \geq M$ is an increasing function with respect to both N_1 and M as defined in (34).

Proof: Please refer to Appendix B. ■

$R_h(N_1, E_1)$ is the average power of the MISO channel when the “best” out of the N_1 independent sub-band channels is selected. It can be easily verified that $R_h(N_1, E_1)$ increases with both N_1 and E_1 , as expected.

Lemma 2: The LMMSE estimator $\hat{\mathbf{h}}_{n^*}$ of \mathbf{h}_{n^*} based on (14) is given by

$$\hat{\mathbf{h}}_{n^*} = \frac{\sqrt{E_2} R_h(N_1, E_1)}{E_2 R_h(N_1, E_1) + N_0 M} \mathbf{y}_{n^*}^{\text{II}}. \quad (16)$$

Define the channel estimation error as $\tilde{\mathbf{h}}_{n^*} \triangleq \mathbf{h}_{n^*} - \hat{\mathbf{h}}_{n^*}$. We also have

$$\mathbb{E} \left[\|\tilde{\mathbf{h}}_{n^*}\|^2 \right] = \frac{N_0 M R_h(N_1, E_1)}{E_2 R_h(N_1, E_1) + N_0 M}, \quad (17)$$

$$\mathbb{E} \left[\|\hat{\mathbf{h}}_{n^*}\|^2 \right] = \frac{E_2 R_h^2(N_1, E_1)}{E_2 R_h(N_1, E_1) + N_0 M}, \quad (18)$$

$$\mathbb{E} \left[\tilde{\mathbf{h}}_{n^*}^H \hat{\mathbf{h}}_{n^*} \right] = 0. \quad (19)$$

Proof: Please refer to Appendix C. ■

B. Net Harvested Energy Maximization

After the two-phase training, energy beamforming is performed by the ET over sub-band n^* based on the estimated channel $\hat{\mathbf{h}}_{n^*}$ during the remaining time of $T - \tau_1 - \tau_2$ seconds. According to (8), we set $\mathbf{s}_{n^*} = \sqrt{P_f} \hat{\mathbf{h}}_{n^*} / \|\hat{\mathbf{h}}_{n^*}\|$.

The resulting energy harvested at the ER can be expressed as²

$$\hat{Q} = \eta T P_f \frac{|\mathbf{h}_{n^*}^H \hat{\mathbf{h}}_{n^*}|^2}{\|\hat{\mathbf{h}}_{n^*}\|^2} \quad (20)$$

$$= \eta T P_f \left(\|\hat{\mathbf{h}}_{n^*}\|^2 + \frac{|\tilde{\mathbf{h}}_{n^*}^H \hat{\mathbf{h}}_{n^*}|^2}{\|\hat{\mathbf{h}}_{n^*}\|^2} + \tilde{\mathbf{h}}_{n^*}^H \hat{\mathbf{h}}_{n^*} + \hat{\mathbf{h}}_{n^*}^H \tilde{\mathbf{h}}_{n^*} \right), \quad (21)$$

¹In principle, \mathbf{h}_{n^*} can be estimated based on both observations $\mathbf{y}_{n^*}^{\text{I}}$ and $\mathbf{y}_{n^*}^{\text{II}}$. To simplify the processing of multi-band energy detection in phase I training, we assume that $\mathbf{y}_{n^*}^{\text{I}}$ is only used for estimating $\|\mathbf{h}_{n^*}\|^2$ while only $\mathbf{y}_{n^*}^{\text{II}}$ is used for estimating \mathbf{h}_{n^*} .

²We assume that T is sufficiently large so that $T \gg \tau_1 + \tau_2$; as a result, the time overhead for channel training is ignored (but energy cost of channel training remains).

where we have used the identity $\mathbf{h}_{n^*} = \hat{\mathbf{h}}_{n^*} + \tilde{\mathbf{h}}_{n^*}$ in (21). The average harvested energy at the ER is then obtained as

$$\begin{aligned}\bar{Q}(N_1, E_1, E_2) &= \mathbb{E} \left[\hat{Q} \right] \\ &= \eta TP_f R_h(N_1, E_1) \left(1 - \frac{(M-1)N_0}{E_2 R_h(N_1, E_1) + N_0 M} \right),\end{aligned}\quad (22)$$

where we have used the results in (17)-(19).

It is observed from (22) that the average harvested energy is given by a difference of two terms. The first term, $\eta TP_f R_h$, is the average harvested energy when energy beamforming is based on the perfect knowledge of \mathbf{h}_{n^*} , with the best sub-band n^* determined via phase I training. The second term can be interpreted as the loss in energy beamforming performance due to the error in the estimated MISO channel $\hat{\mathbf{h}}_{n^*}$ in phase II training. As $E_2/N_0 \rightarrow \infty$, \mathbf{h}_{n^*} can be perfectly estimated and hence the second term in (22) vanishes.

The *net* average harvested energy at the ER, which is the average harvested energy offset by that used for sending training signals in the two phases, is given by

$$\bar{Q}_{\text{net}}(N_1, E_1, E_2) = \bar{Q}(N_1, E_1, E_2) - E_1 N_1 - E_2. \quad (23)$$

The problem of finding the optimal training design to maximize \bar{Q}_{net} can be formulated as

$$\begin{aligned}(\text{P1}) : \quad & \max_{E_1 \geq 0, E_2 \geq 0, N_1} \bar{Q}_{\text{net}}(N_1, E_1, E_2) \\ & \text{subject to } N_1 \in \{1, \dots, N\}.\end{aligned}$$

IV. OPTIMAL TRAINING DESIGN

To find the optimal solution to (P1), we first obtain the optimal training energy E_2 with N_1 and E_1 fixed. By discarding irrelevant terms, the resulting sub-problem can be formulated as

$$\min_{E_2 \geq 0} \frac{(M-1)N_0 \eta TP_f R_h(N_1, E_1)}{E_2 R_h(N_1, E_1) + N_0 M} + E_2, \quad (24)$$

which is convex with the optimal solution given by

$$E_2^*(N_1, E_1) = \left[\sqrt{\eta TP_f (M-1)N_0} - \frac{N_0 M}{R_h(N_1, E_1)} \right]^+, \quad (25)$$

where $[x]^+ \triangleq \max\{x, 0\}$. By substituting $E_2^*(N_1, E_1)$ into (22), the resulting average net energy as a function of N_1 and E_1 can be expressed as

$$\bar{Q}_{\text{net}}(N_1, E_1) = \begin{cases} \eta TP_f R_h(N_1, E_1) + \frac{N_0 M}{R_h(N_1, E_1)} - E_1 N_1 - 2\sqrt{\eta TP_f (M-1)N_0}, & \text{if } R_h(N_1, E_1) > \alpha, \\ \frac{\eta TP_f R_h(N_1, E_1)}{M} - E_1 N_1, & \text{otherwise,} \end{cases} \quad (26)$$

where $\alpha \triangleq \sqrt{N_0 M} / \eta TP_f (M-1)$.

As a result, (P1) reduces to

$$\begin{aligned}& \max_{E_1 \geq 0, N_1} \bar{Q}_{\text{net}}(N_1, E_1) \\ & \text{subject to } N_1 \in \{1, \dots, N\}.\end{aligned}\quad (27)$$

To find the optimal solution to problem (27), we first obtain the optimal E_1 with N_1 fixed by solving

$$\max_{E_1 \geq 0} \bar{Q}_{\text{net}}(N_1, E_1). \quad (28)$$

It can be obtained from (15) that for any fixed N_1 , as the training energy E_1 varies from 0 to ∞ , $R_h(N_1, E_1)$ monotonically increases from βM to $\beta G(N_1, M)$, i.e.,

$$\beta M \leq R_h(N_1, E_1) \leq \beta G(N_1, M), \quad \forall E_1 \geq 0. \quad (29)$$

As a result, problem (28) can be solved by separately considering the following three cases:

Case 1: $\alpha \geq \beta G(N_1, M)$: In this case, we have $R_h(N_1, E_1) \leq \alpha$ and hence $\bar{Q}_{\text{net}}(N_1, E_1) = \eta T P_f R_h(N_1, E_1) / M - E_1 N_1, \forall E_1 \geq 0$. By substituting $R_h(N_1, E_1)$ with (15), problem (28) reduces to

$$\max_{E_1 \geq 0} \eta T P_f \beta \frac{\beta E_1 G(N_1, M) / M + N_0}{\beta E_1 + N_0} - E_1 N_1, \quad (30)$$

which is convex with the optimal solution given by

$$E_1^*(N_1) = \left[\sqrt{\frac{\eta T P_f N_0 (G(N_1, M) / M - 1)}{N_1}} - \frac{N_0}{\beta} \right]^+.$$

Case 2: $\alpha \leq \beta M$: In this case, $R_h(N_1, E_1) > \alpha, \forall E_1 \geq 0$. Therefore, $\bar{Q}_{\text{net}}(N_1, E_1)$ is given by the first expression of (26). After discarding irrelevant terms, problem (28) can be explicitly written as

$$\max_{E_1 \geq 0} \eta T P_f \frac{\beta^2 E_1 G(N_1, M) + \beta N_0 M}{\beta E_1 + N_0} + \frac{N_0 M (\beta E_1 + N_0)}{\beta^2 E_1 G(N_1, M) + \beta N_0 M} - E_1 N_1. \quad (31)$$

Problem (31) is non-convex in general. However, as the objective function is continuously differentiable, the optimal solution is given either by $E_1 = 0$, or by one of the positive stationary points satisfying $\frac{\partial \bar{Q}_{\text{net}}(N_1, E_1)}{\partial E_1} = 0$, which can be easily determined by solving a quartic equation.

Case 3: $\beta M < \alpha < \beta G(N_1, M)$: In this case, it can be obtained that $\bar{Q}_{\text{net}}(N_1, E_1)$ in (26) can be explicitly expressed as (32) shown at the top of the next page,

$$\bar{Q}_{\text{net}}(N_1, E_1) = \begin{cases} \eta T P_f \frac{\beta^2 E_1 G(N_1, M) / M + \beta N_0}{\beta E_1 + N_0} - E_1 N_1, & \text{if } E_1 \leq E_0, \\ \eta T P_f \frac{\beta^2 E_1 G(N_1, M) + \beta N_0 M}{\beta E_1 + N_0} + \frac{N_0 M (\beta E_1 + N_0)}{\beta^2 E_1 G(N_1, M) + \beta N_0 M} - E_1 N_1 - 2\sqrt{\eta T P_f (M - 1) N_0}, & \text{otherwise,} \end{cases} \quad (32)$$

where $E_0 \triangleq \frac{N_0(\alpha - \beta M)}{\beta(\beta G - \alpha)}$. Similar to that in Case 2, the optimal solution to problem (28) with $\bar{Q}_{\text{net}}(N_1, E_1)$ given in (32) is given either by the boundary point $E_1 = 0$ or one of the stationary points, which can be readily determined by solving a quartic equation.

With problem (28) solved for all three cases as discussed above, the corresponding optimal value $\bar{Q}_{\text{net}}^*(N_1)$ as a function of N_1 can be readily determined. Therefore, finding the optimal solution to problem (27) and that to the original problem (P1) reduces to determining the optimal number of sub-bands to be trained, i.e., $N_1^* = \arg \max_{1 \leq N_1 \leq N} \bar{Q}_{\text{net}}^*(N_1)$, which can be easily found by exhaustive search.

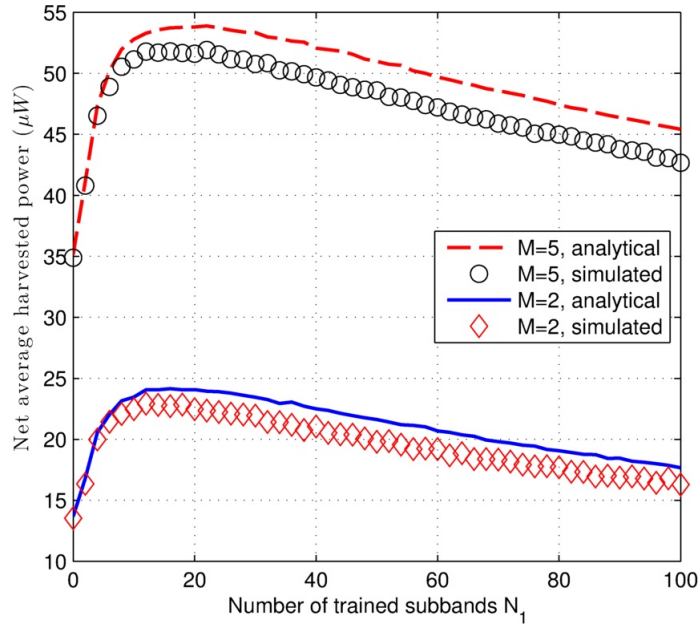


Fig. 3. Net average harvested power versus the number of trained sub-bands N_1 .

V. NUMERICAL RESULTS

In this section, numerical examples are provided to corroborate our study. To model the frequency-selective channel, we assume a multi-path power delay profile with the exponential distribution $A(\tau) = \frac{1}{\sigma_{\text{rms}}} e^{-\tau/\sigma_{\text{rms}}}$, $\tau \geq 0$, where σ_{rms} denotes the root-mean-square (rms) delay spread. We set $\sigma_{\text{rms}} = 1\mu\text{s}$ so that the 50% channel coherence bandwidth, i.e., the frequency separation for which the amplitude correlation is 0.5, is $B_c = \frac{1}{2\pi\sigma_{\text{rms}}} \approx 160$ kHz. The total available spectrum for energy transmission is $B = 10\text{MHz}$, which is divided into $N = 100$ sub-bands each with bandwidth $B_s = 100\text{kHz}$. The average power attenuation between the ET and the ER is assumed to be 50 dB, i.e., $\beta = 10^{-5}$, and the transmission power at the ET is set as $P_f = 1\text{watt}$ or 30dBm. The power spectrum density of the training noise received at the ET is $N_0 = -120\text{dBm/Hz}$. The energy harvesting efficiency at the ER is set as $\eta = 0.8$.

In Fig. 3, by varying the number of sub-bands N_1 that are trained in phase I, the net average harvested power achieved by the proposed two-phase training scheme is plotted for $M = 5$ and $M = 2$, where the average is taken over 10000 random channel realizations. The channel block length is set as $T = 0.5\text{ms}$. The analytical result obtained in Section IV, i.e., $\bar{Q}_{\text{net}}^*(N_1)/T$ with $\bar{Q}_{\text{net}}^*(N_1)$ denoting the optimal value of problem (28), is also shown in Fig. 3. It is observed that the simulation and analytical results match well for small and moderate N_1 values, for which the assumption of independent channels between any two sub-bands as in Lemma 1 is more valid. Furthermore, Fig. 3 shows that there is an optimal number of sub-bands trained to maximize the net harvested energy, as a result of the trade-off between achieving more frequency-diversity gain (with larger N_1) and reducing the training energy ($E_1 N_1$ in phase I).

In Fig. 4, the optimal training energy per sub-band E_1 and E_2 in phases I and II, respectively, are plotted against

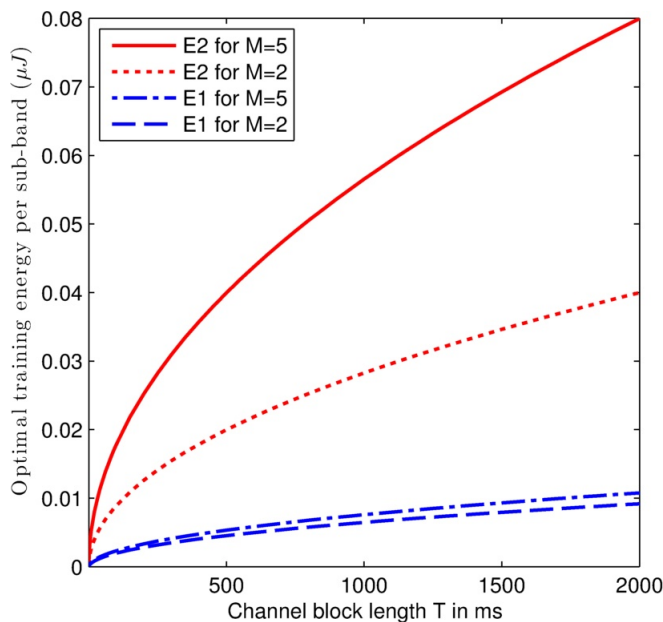


Fig. 4. Optimal training energy E_1 and E_2 versus block length T for $M = 2$ and $M = 5$.

the channel block length T , with T ranging from 0.1ms to 2 seconds. It is observed that E_1 and E_2 both increase with T , as expected. Furthermore, for both setups, E_2 is significantly larger than E_1 , since in phase II, only the selected sub-band needs to be further trained, whereas the training energy in phase I needs to be distributed over N_1 sub-bands to exploit the frequency-diversity.

In Fig. 5, the net average harvested power based on the proposed two-phase training scheme is plotted against block length T with $M = 5$. The following four benchmark schemes are also included for comparison: i) perfect CSIT, whose average harvested energy can be obtained as $\bar{Q}_{\max} = \eta T P_f \beta G(N, M)$; ii) no CSIT, with $\bar{Q}_{\text{noCSIT}} = \eta T P_f \beta$; iii) phase I training only, which corresponds to the special case of the two-phase training scheme with $E_2 = 0$; iv) phase II training only, which corresponds to the two-phase scheme with $E_1 = 0$. It is observed from Fig. 5 that the proposed two-phase training scheme approaches to the performance upper bound with perfect CSIT as T increases, and significantly outperforms the other three benchmark schemes. It is also worth noting that for multi-antenna frequency-selective WET systems, exploiting either frequency-diversity gain or beamforming gain alone is far from optimal; instead, a good balance between these two gains as achieved in the proposed two-phase training optimization is needed.

VI. CONCLUSION

This paper studies the optimal training design for a MISO WET system in frequency-selective channels. By exploiting channel reciprocity, a two-phase training scheme is proposed to exploit the frequency-diversity and energy-beamforming gains, respectively. A closed-form expression has been derived for the average harvested energy. The optimal training scheme, including the number of independent sub-bands trained and the energy allocated for each of the two training phases, is derived. Numerical results are provided to validate our analysis and show the

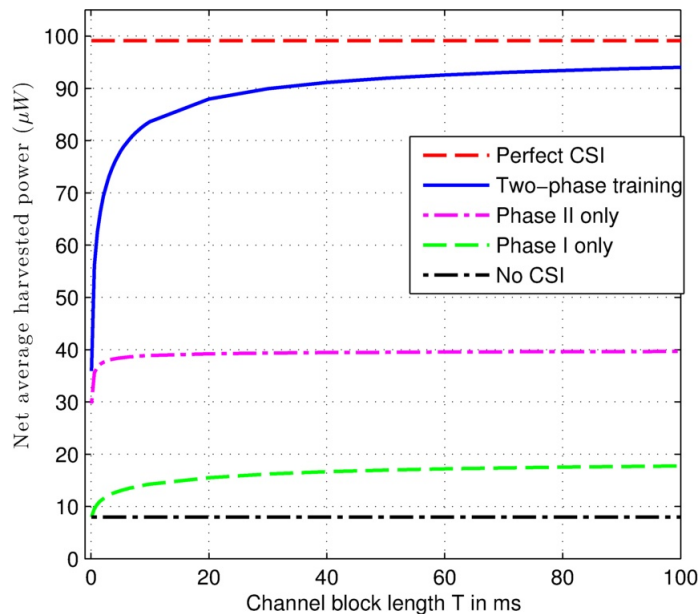


Fig. 5. Net average harvested power with $M = 5$.

effectiveness of the proposed scheme by optimally balancing the achievable diversity and beamforming gains with limited training energy.

APPENDIX A

A USEFUL LEMMA

Lemma 3: Let $\mathbf{v}_1, \dots, \mathbf{v}_{N_1} \in \mathbb{C}^{M \times 1}$ be N_1 i.i.d. zero-mean CSCG random vectors distributed as $\mathbf{v}_n \sim \mathcal{CN}(\mathbf{0}, \sigma_v^2 \mathbf{I}_M)$, $\forall n$. Then we have

$$\mathbb{E} \left[\max_{n=1, \dots, N_1} \|\mathbf{v}_n\|^2 \right] = \sigma_v^2 G(N_1, M), \quad (33)$$

where $G(N_1, M)$ is a function of N_1 and M given by

$$G(N_1, M) = \sum_{n=1}^{N_1} \binom{N_1}{n} (-1)^{n+1} c_n, \quad (34)$$

with

$$c_n = \sum_{k_0 + \dots + k_{M-1} = n} \binom{n}{k_0, \dots, k_{M-1}} \left(\prod_{m=0}^{M-1} \frac{1}{(m!)^{k_m}} \right) \left(\sum_{m=0}^{M-1} m k_m \right)! \frac{1}{n^{1 + \sum_{m=0}^{M-1} m k_m}}. \quad (35)$$

Note that in (35), the summation is taken over all sequences of non-negative integer indices k_0 to k_{M-1} with the sum equal to n , and the coefficients $\binom{n}{k_0, \dots, k_{M-1}}$ are known as multinomial coefficients, which can be computed as

$$\binom{n}{k_0, \dots, k_{M-1}} = \frac{n!}{k_0! \dots k_{M-1}!}. \quad (36)$$

Proof: Define the random variables $V_n \triangleq \|\mathbf{v}_n\|^2$, $n = 1, \dots, N_1$. It then follows that V_1, \dots, V_{N_1} are i.i.d. Erlang distributed with shape parameter M and rate $\lambda = 1/\sigma_v^2$, whose cumulative distribution function (CDF) is given by

$$F_{V_n}(v) = \Pr(V_n \leq v) = 1 - \sum_{m=0}^{M-1} \frac{1}{m!} e^{-\lambda v} (\lambda v)^m, \quad \forall n. \quad (37)$$

Let $V \triangleq \max_{n=1, \dots, N_1} V_n$. Then the CDF of V can be obtained as

$$F_V(v) = \Pr(v_1 \leq v, \dots, v_{N_1} \leq v) = \prod_{n=1}^{N_1} F_{V_n}(v) = \left(1 - \sum_{m=0}^{M-1} \frac{1}{m!} e^{-\lambda v} (\lambda v)^m \right)^{N_1}. \quad (38)$$

With binomial expansion, the expectation of V can be expressed as

$$\mathbb{E}[V] = \int_0^\infty (1 - F_V(v)) dv \quad (39)$$

$$= \sum_{n=1}^{N_1} \binom{N_1}{n} (-1)^{n+1} a_n, \quad (40)$$

where

$$a_n = \int_0^\infty e^{-\lambda n v} \left(\sum_{m=0}^{M-1} \frac{1}{m!} (\lambda v)^m \right)^n dv \quad (41)$$

$$= \sum_{k_0 + \dots + k_{M-1} = n} \binom{n}{k_0, \dots, k_{M-1}} \left(\prod_{m=0}^{M-1} \frac{1}{(m!)^{k_m}} \right) \lambda^{\sum_{m=0}^{M-1} m k_m} \int_0^\infty e^{-\lambda n v} v^{\sum_{m=0}^{M-1} m k_m} dv \quad (42)$$

$$= \frac{1}{\lambda} c_n = \sigma_v^2 c_n, \quad (43)$$

where (42) follows from the multinomial expansion theorem, and (43) follows from the integral identity $\int_0^\infty x^n e^{-\mu x} dx = n! \mu^{-n-1}$ ([13]3.351). The result in (33) can then be obtained by substituting (43) into (40).

Furthermore, it can be directly obtained from (33) that $G(N_1, M)$ is an increasing function with respect to both N_1 and M , with $G(1, M) = M$, $\forall M$.

This completes the proof of Lemma 3. ■

APPENDIX B

PROOF OF LEMMA 1

Note that in the absence of training phase I or only one sub-band is trained ($N_1 = 1$), the distribution of \mathbf{h}_{n^*} is simply given by (1). In this case, $\mathbb{E}[\|\mathbf{h}_{n^*}\|^2] = \beta M$, which is equal to that obtained by evaluating (15) with $E_1 = 0$ or $N_1 = 1$. For the general scenario with $N_1 \geq 2$, n^* is determined by the sub-band with the maximum total received energy as in (13). As a consequence, the corresponding channel vector \mathbf{h}_{n^*} statistically depends on all the N_1 channels $\mathbf{h}_1, \dots, \mathbf{h}_{N_1}$ via (12) and (13). To exploit such a relationship, we first show the following result:

Lemma 4: The input-output relationship in (12) is statistically equivalent to

$$\mathbf{h}_n = \frac{\beta\sqrt{E_1}}{\beta E_1 + N_0} \mathbf{y}_n^I + \sqrt{\frac{\beta N_0}{\beta E_1 + N_0}} \mathbf{t}_n, \quad n = 1, \dots, N_1, \quad (44)$$

where $\mathbf{t}_n \sim \mathcal{CN}(\mathbf{0}, \mathbf{I}_M)$ is a CSCG random vector independent of \mathbf{y}_n^I , i.e.,

$$\mathbb{E} [\mathbf{y}_n^I \mathbf{t}_n^H] = \mathbf{0}, \quad n = 1, \dots, N_1. \quad (45)$$

Proof: It follows from (1) and (12) that \mathbf{y}_n^I is a CSCG random vector distributed as

$$\mathbf{y}_n^I \sim \mathcal{CN}(\mathbf{0}, (\beta E_1 + N_0) \mathbf{I}_M), \quad \forall n. \quad (46)$$

Furthermore, the cross-correlation between \mathbf{h}_n and \mathbf{y}_n^I is

$$\mathbb{E} [\mathbf{y}_n^I \mathbf{h}_n^H] = \beta \sqrt{E_1} \mathbf{I}_M. \quad (47)$$

To prove Lemma 4, it is sufficient to show that the random vector \mathbf{h}_n obtained by (44) has the same distribution as (1), and also has the same cross-correlation with \mathbf{y}_n^I as (47). The desired results can be easily verified based on (44) and (46). ■

By applying Lemma 4, we can obtain the following result

$$\mathbb{E} [\|\mathbf{h}_{n^*}\|^2] = \frac{\beta^2 E_1}{(\beta E_1 + N_0)^2} \mathbb{E} [\|\mathbf{y}_{n^*}^I\|^2] + \frac{\beta N_0 M}{\beta E_1 + N_0} \quad (48)$$

$$= \frac{\beta^2 E_1}{(\beta E_1 + N_0)^2} \mathbb{E} \left[\max_{n=1, \dots, N_1} \|\mathbf{y}_n^I\|^2 \right] + \frac{\beta N_0 M}{\beta E_1 + N_0} \quad (49)$$

$$= \frac{\beta^2 E_1 G(N_1, M) + \beta N_0 M}{\beta E_1 + N_0}, \quad (50)$$

where (49) follows from (13), and (50) is true due to Lemma 3 and (46).

This completes the proof of Lemma 1.

APPENDIX C

PROOF OF LEMMA 2

Since both \mathbf{h}_{n^*} and $y_{n^*}^{\text{II}}$ are zero-mean random vectors with i.i.d entries, the LMMSE estimator can be expressed as $\hat{\mathbf{h}}_{n^*} = b \mathbf{y}_{n^*}^{\text{II}}$, with b a complex-valued parameter to be determined. The corresponding MSE can be expressed as

$$e = \mathbb{E} \left[\|\tilde{\mathbf{h}}_{n^*}\|^2 \right] = \mathbb{E} \left[\left\| (1 - b\sqrt{E_2}) \mathbf{h}_{n^*} - b \mathbf{z}_{n^*}^{\text{II}} \right\|^2 \right] \quad (51)$$

$$= \left| 1 - b\sqrt{E_2} \right|^2 R_h(N_1, E_1) + |b|^2 N_0 M \quad (52)$$

$$= |b|^2 (E_2 R_h(N_1, E_1) + N_0 M) - (b + b^*) \sqrt{E_2} R_h(N_1, E_1) + R_h(N_1, E_1). \quad (53)$$

By setting the derivative of e with respect to b^* equals to zero, the optimal coefficient b can be obtained as

$$b = \frac{\sqrt{E_2} R_h(N_1, E_1)}{E_2 R_h(N_1, E_1) + N_0 M}. \quad (54)$$

The resulting MMSE can be obtained accordingly.

Furthermore, the following result can be obtained

$$\mathbb{E} \left[\|\hat{\mathbf{h}}_{n^*}\|^2 \right] = |b|^2 \mathbb{E} \left[\|\mathbf{y}_{n^*}^{\Pi}\|^2 \right] = \frac{E_2 R_h^2(N_1, E_1)}{E_2 R_h(N_1, E_1) + N_0 M}. \quad (55)$$

To show that $\mathbb{E} \left[\tilde{\mathbf{h}}_{n^*}^H \hat{\mathbf{h}}_{n^*} \right] = 0$, we will use the following result

$$\mathbb{E} \left[\mathbf{h}_{n^*}^H \hat{\mathbf{h}}_{n^*} \right] = b \mathbb{E} \left[\mathbf{h}_{n^*}^H \mathbf{y}_{n^*}^{\Pi} \right] = \frac{E_2 R_h^2(N_1, E_1)}{E_2 R_h(N_1, E_1) + N_0 M} = \mathbb{E} \left[\|\hat{\mathbf{h}}_{n^*}\|^2 \right]. \quad (56)$$

Therefore, we have

$$\mathbb{E} \left[\tilde{\mathbf{h}}_{n^*}^H \hat{\mathbf{h}}_{n^*} \right] = \mathbb{E} \left[\mathbf{h}_{n^*}^H \hat{\mathbf{h}}_{n^*} \right] - \mathbb{E} \left[\|\hat{\mathbf{h}}_{n^*}\|^2 \right] = 0, \quad (57)$$

where we have used the identity $\tilde{\mathbf{h}}_{n^*} = \mathbf{h}_{n^*} - \hat{\mathbf{h}}_{n^*}$.

This completes the proof of Lemma 2.

REFERENCES

- [1] H. J. Visser and R. J. M. Vullers, "RF energy harvesting and transport for wireless sensor network applications: Principles and requirements," *Proceedings of the IEEE*, vol. 101, no. 6, pp. 1410–1423, Jun. 2013.
- [2] S. Bi, C. K. Ho, and R. Zhang, "Wireless powered communication: opportunities and challenges," submitted to *IEEE Commun. Mag.*, available online at <http://arxiv.org/abs/1408.2335>.
- [3] R. Zhang and C.-K. Ho, "MIMO broadcasting for simultaneous wireless information and power transfer," *IEEE Trans. Wireless Commun.*, vol. 12, no. 5, pp. 1989–2001, May 2013.
- [4] L. Lu, G. Y. Li, A. L. Swindlehurst, A. Ashikhin, and R. Zhang, "An overview of massive MIMO: benefits and challenges," to appear in *IEEE J. Sel. Topics Signal Process.*
- [5] P. Grover and A. Sahai, "Shannon meets tesla: Wireless information and power transfer," in *Int. Symp. on Inf. Theory*, Jun. 2010, pp. 2363–2367.
- [6] D. W. K. Ng, E. S. Lo, and R. Schober, "Wireless information and power transfer: Energy efficiency optimization in OFDMA systems," *IEEE Trans. Wireless Commun.*, vol. 12, no. 12, pp. 6352–6370, Dec. 2013.
- [7] X. Zhou, R. Zhang, and C. K. Ho, "Wireless information and power transfer in multiuser OFDM systems," *IEEE Trans. Wireless Commun.*, vol. 13, no. 4, pp. 2282–2294, Apr. 2014.
- [8] D. J. Love, R. W. Heath Jr., V. K. N. Lau, D. Gesbert, B. D. Rao, and M. Andrews, "An overview of limited feedback in wireless communication systems," *IEEE J. Sel. Areas Commun.*, vol. 26, no. 8, pp. 1341–1365, Oct. 2008.
- [9] G. Yang, C. K. Ho, and Y.-L. Guan, "Dynamic resource allocation for multiple-antenna wireless power transfer," *IEEE Trans. Signal Process.*, vol. 62, no. 14, pp. 3565 – 3577, Jun. 2014.
- [10] J. Xu and R. Zhang, "Energy beamforming with one-bit feedback," to appear in *IEEE Trans. Signal Process.*, available online at <http://arxiv.org/abs/1312.1444>.
- [11] Y. Zeng and R. Zhang, "Optimal training for wireless energy transfer," submitted to *IEEE Trans. Commun.*, available online at <http://arxiv.org/abs/1403.7870>.
- [12] X. Zhou, R. Zhang, and C. K. Ho, "Wireless information and power transfer: architecture design and rate-energy tradeoff," *IEEE Trans. Commun.*, vol. 61, no. 11, pp. 4757–4767, Nov. 2013.
- [13] I. Gradshteyn and I. M. Ryzhik, *Table of integrals, series and products*, 7th ed. Elsevier Academic Pres, 2007.